PDCD4–MAPK–NF-κB Positive Loop Simultaneously Promotes Microglia Activation and Neuron Apoptosis During Neuroinflammation

Quan Chen
Nantong City No 1 People's Hospital and Second Affiliated Hospital of Nantong University
Hongjian Lu
Nantong City No 1 People's Hospital and Second Affiliated Hospital of Nantong University
Chengwei Duan
Nantong City No 1 People's Hospital and Second Affiliated Hospital of Nantong University
Xiangyang Zhu
Nantong City No 1 People's Hospital and Second Affiliated Hospital of Nantong University
Yi Zhang
Nantong City No 1 People's Hospital and Second Affiliated Hospital of Nantong University
Mengmeng Li
Nantong City No 1 People's Hospital and Second Affiliated Hospital of Nantong University
Dongmei Zhang (zdm_ntyy@163.com)
Nantong City No 1 People's Hospital and Second Affiliated Hospital of Nantong University
https://orcid.org/0000-0002-4132-7363

Research Article

Keywords: programmed cell death factor 4 (PDCD4), mitogen-activated protein kinases (MAPKs), nuclear factor-κB (NF-κB), microglia, neuroinflammation, neuron apoptosis

Posted Date: March 31st, 2021

DOI: https://doi.org/10.21203/rs.3.rs-348335/v1

Abstract

Neuroinflammation and neuron injury are common features of the central nervous system (CNS) diseases. It is of great significance to identify their shared regulatory mechanisms and explore the potential therapeutic targets. Programmed cell death factor 4 (PDCD4), an apoptosis-related molecule, extensively participates in tumorigenesis and inflammatory diseases, but its expression and biological function during CNS neuroinflammation remain unclear. In the present study, utilizing the lipopolysaccharide (LPS)-induced neuroinflammation model in mice, we reported an elevated expression of PDCD4 both in injured neurons and activated microglia of the inflamed brain. A similar change in PDCD4 expression was observed in vitro in the microglial activation model. Silencing PDCD4 by shRNA significantly inhibited the phosphorylation of MAPKs (p38, ERK, and JNK), prevented the phosphorylation and nuclear translocation of NF-κB p65, and thus attenuated the LPS-induced microglial inflammatory activation. Interestingly, LPS also required the MAPK/NF-κB signaling activation to boost PDCD4 expression in microglia, indicating the presence of a positive loop. Moreover, a persistent elevation of PDCD4 expression was detected in the H_2O_2-induced neuronal oxidative damage model. Knocking down PDCD4 significantly inhibited the expression of proapoptotic protein BAX, suggesting the proapoptotic activity of PDCD4 in neurons. Taken together, our data indicated that PDCD4 may serve as a hub regulatory molecule that simultaneously promotes the microglial inflammatory activation and the oxidative stress-induced neuronal apoptosis within CNS. The microglial PDCD4–MAPK–NF-κB positive feedback loop may exaggerate the vicious cycle of neuroinflammation and neuronal injury and thus may become a potential therapeutic target for neuroinflammatory diseases.

Introduction

Neuroinflammation, an inflammatory reaction occurring within the central nervous system (CNS), extensively participates in pathological processes in the CNS[1-3]. Microglia, the principal resident immune cells in CNS that account for approximately 10% of brain parenchymal cells, act as the main executor of neuroinflammation[4-6]. Under physiological conditions, microglia secrete multiple neurotrophic factors, dynamically monitor synaptic functions, and clear dead cell debris to maintain brain homeostasis. Stimulated by pathogen-associated molecular patterns (PAMPs) following pathogen infection, or by damage-associated molecular patterns (DAMPs) during ischemia, trauma, or neurodegeneration, microglia proliferate, migrate to the damaged area, and act as the first line of defense in the brain[7,8]. Apart from the neuroprotective effects, microglia have proinflammatory functions, considering that they are the main source of interleukin (IL)-1β, IL-6, tumor necrosis factor-α (TNF-α), chemokines, reactive oxygen species (ROS), and nitric oxide (NO), which further exacerbate the neuroinflammation and result in the subsequent neuronal injury[9-12].

Accumulating evidence suggests that neuroinflammation and neuron injury can form a vicious cycle to promote neuropathological disorders[13]. For example, we previously reported that soluble HSP60, which is released by the injured neurons, can act as extracellular DAMPs, combining with the microglial receptor LOX-1 and driving neuroinflammation[14][15]. The mitogen-activated protein kinases (MAPKs) family,

including intracellular signal-regulated kinase 1/2 (ERK1/2), the c-Jun N-terminal (JNK), and p38 MAPK, is the backbone of the major proinflammatory signaling pathway within microglia, which can be activated by various PAMPs (such as LPS) or DAMPs (such as sHSP60 or the conditioned medium collected from the injured neurons)[15][16]. After the activation, MAPKs subsequently trigger the phosphorylation and nuclear translocatin of transcription factors, such as nuclear factor-κB (NF-κB) or activating protein-1 (AP-1), thereby enhancing the transcription of the downstream proinflammatory genes[15][16]. Although a large number of studies have focused on the inflammatory activation of microglia, the exact molecular mechanism has not been fully elucidated. Considering the close interaction of neuroinflammation and neuronal injury, it is of great significance to identify their shared regulatory molecule, analyze their internal relationship, and explore the potential therapeutic targets.

Human programmed cell death factor 4 (PDCD4) gene, discovered in 1999, is located on chromosome 3q21.3 with a total length of 28212bp and encodes a protein containing 496 amino acid residues[17][18]. Based on proapoptotic and cell-cycle inhibiting activity of PDCD4, intensive efforts have been invested to clarify its role as a tumor suppressor[19][20]. PDCD4 exerts its antineoplastic effects by promoting cellular apoptosis and inhibiting malignant transformation, cellular proliferation, invasion, and metastasis[19][20][21] Mechanistically, PDCD4 binds to eIF4A/E to inhibit the RNA helicase activity or directly interacts with the target mRNAs to block protein translation[18][19]. PDCD4 can also combine with certain cytoplasmic proteins or interact with some transcription factors to modulate the target gene transcription[18][19].

Besides the tumor-suppressive activity, PDCD4 is also widely expressed in immune cells. It closely participates in inflammatory responses, but its role during inflammation is still uncertain. The available conflicting evidence showed both the proinflammatory and anti-inflammatory effects of PDCD4 under different experimental conditions[18][19]. For example, PDCD4 deficiency protected mice against diet-induced obesity, inflammation in white adipose tissue, and insulin resistance via restoring LXR-α expression[22]. LPS required PDCD4 to induce NF-κB activation and IL-6 expression, and mice deficient in PDCD4 were protected from LPS-induced death[23]. In contrast, other studies reported that PDCD4 knockout mice displayed upregulation of proinflammatory cytokines (such as IL-6) and enhanced activation of the proinflammatory STAT3 activation in the experimental colitis model[24]. The expression and biological function of PDCD4 in CNS have been rarely reported, especially in relation to microglial activation and neuroinflammation[25].

In this study, we analyzed the temporal-spatial pattern of PDCD4 expression in the classical LPS-induced neuroinflammation model in mice and detected its association with microglial activation and neuronal apoptosis for the first time. Utilizing an in vitro microglial activation model stimulated by LPS, we demonstrated the proinflammatory function of PDCD4 in microglia; we also observed its proapoptotic activity in the oxidative damaged neuronal model. More importantly, our data suggested the existence of a PDCD4–MAPK–NF-κB positive feedback loop to promote the microglial activation and neuronal injury during neuroinflammation.

Materials And Methods

Animals and Treatments

Six- to eight-week-old male C57BL/6 (n = 63) mice were purchased from the Experimental Animal Center of Nantong University (China) and then randomly assigned into seven groups, including one control group and six experimental groups. The experimental mice had a free access to food and water for 7 days in a 12-hour light–dark cycle temperature-controlled environment (21°C). To establish the CNS inflammation model[26], the mice were intraperitoneally injected with 9 mg/kg of LPS (Escherichia coli O111-B4, Sigma, St. Louis, MO, USA), whereas the same amount of normal saline was injected in the control group. The mice were anesthetized at a specific time point after the injection to harvest the brain tissue[27]. All of the animal experiments were performed in accordance with the protocol approved by the Institutional Animal Ethics Committee. All efforts were made to minimize the number of animals and their suffering in this experiment.

Cell Cultures and Stimulation

The mouse microglia cell line BV2 and the mouse hippocampal neuron cell line HT22 were cultured with 10% (v/v) fetal bovine serum and 0.1% penicillin–streptomycin in DMEM medium (C119955OOBT, Gibco, China) under an atmosphere of a humidified air and 5% CO2 at 37°C. To establish the microglial activation model, 100 ng/mL LPS (L4391, Sigma, USA) was used to stimulate BV2 cells at different time points (0 h, 1 h, 3 h, 6 h, 12 h, and 24 h). To mimic the oxidative damage of neurons in vitro, HT22 cells were exposed to various concentrations of H_2O_2 (50, 100, 200, 400, 500, and 100 μM) for 24 h. Then, we selected the appropriate concentration of H_2O_2 (400 μM) to stimulate HT22 cells at different time points.

Quantitative Real-Time Polymerase Chain Reaction Analysis

Total RNA from mouse brain tissue and BV2 was extracted using TRIzol (15596018, Ambion, USA) and quantified using NanoDrop spectrophotometer (NanoDrop ONE C, Thermo Fisher Scientific, USA). Next, the cDNA synthesis was conducted using 5× PrimeScript RT Master Mix (TaKaRa) in line with the manufacturer's instructions. Quantitative real-time polymerase chain reaction (qRT-PCR) was performed using 2×QuantiNova SYBR Green (QIAGEN) to analyze gene expression on the Bio-Rad CFX Maestro 1.0 system. The relative mRNA expression was analyzed by using the 2-ΔΔCT method, normalized to GAPDH. Primer pair sequences are shown in Table 1.

Table 1

DNA sequences of primers used in PCRs and expected product sizes.

	Forward primer (5'-3')	Reverse primer (5'-3')	Size(bp)
GAPDH	CAAGGTCATCCATGACAACTTTG	GTCCACCACCCTGTTGCTGTAG	496
iNOS	CAAGAGTTTGACCAGAGGACC	TGGAACCACTCGTACTTGGGA	654
IL-6	GCCTTCTTGGGACTGATGCT	TGGAAATTGGGGTAGGAAGGAC	475
IL-1β	TCATTGTGGCTGTGGAGAAG	AGGCCACAGGTATTTTGTCG	333
TNF-α	ACAGAAAGCATGATCCGCGA	TTGCTACGACGTGGGCTAC	286

Immunohistochemistry

Fresh brain tissue was fixed with 4% paraformaldehyde at 4°C overnight, embedded in Tissue-Tek O.C.T compound (SAKURA), and cut into 20-μm-thick sections by cryotome sections (CM1860, Leica, Germany). The immunohistochemistry of the brain sections was performed according to the DAB Detection Kit's instructions (GK600511, Gene Tech, Shanghai, China). After returning to room temperature, the sections were washed with phosphate-buffered saline (PBS). After blocking endogenous peroxidase for 20 min in the dark, the sections were incubated with anti-PDCD4 (1:100, CST, USA) overnight at 4°C. Next, they were incubated with horseradish peroxidase (HRP) at room temperature for 30 min and stained with diaminobenzidine (DAB), followed by gradient dehydration, drying, and resin sealing. The stained sections were observed using a microscope (ECLIPSE Ni-U, Nikon, Japan) on NIS-Elements F 4.6 system.

Immunofluorescence Staining

The brain tissue sections were stained by standard immunohistochemistry procedures. Briefly, the frozen sections were permeabilized in 0.3% Triton-100 for 20 min and blocked with 5% bovine serum albumin (BSA) for 1 h. Next, the sections were incubated at 4°C overnight with the following antibodies, as appropriate: anti-PDCD4 (rabbit, 1:200, 9535, CST, USA), anti-PDCD4 (mouse, 1:100, sc-376430, Santa Cruz, USA), anti-NeuN (mouse, 1:400, MAB377, Millipore, USA), anti-GFAP (mouse, 1:400, G3893, Sigma, USA), anti-Iba1 (rabbit, 1:1000, 019-19741, Wako, Japan), anti-iNOS (rabbit, 1:200, ab178945, Abcam, UK), and anti-Cleaved Caspase-3 (rabbit, 1:200, 9661s, Sigma, USA). Next, the sections were incubated with the proper Alexa secondary antibodies (1:1000, A10042, A21202, A21206, A10037, Thermo Fisher Scientific, USA) at room temperature in the dark for 2 h, and the nuclei were stained with DAPI (Sigma, USA). All the sections were observed using a fluorescence microscope (ECLIPSE Ni-E, Nikon, Japan) on the NIS-Elements D 5.11 system.m

Western Blot

The lysis buffer (RIPA effective lysis solution: PMSF=100:1) was used to lyse and release the proteins from the cells and mouse cerebral cortex tissues at 4°C, and the supernatant was collected after

centrifugation. The protein concentration was determined using the BCA assay (23225, Thermo Fisher, USA). The proper amount of protein samples was subjected to 10% SDS-polyacrylamide gel electrophoresis and transferred to polyvinylidene fluoride (PVDF) membrane (Millipore). The membrane was blocked with 5% skim milk for 2 h, followed by an overnight incubation at 4°C with the specific primary antibodies, including anti-PDCD4 (9535, CST, USA), anti-iNOS (ab178945, Abcam, UK), anti-IL-1β (ab9722, Abcam, UK), anti-GAPDH (60004-10-Ig, Proteintech, China), anti-Cleaved PARP (5625s, CST, USA), anti-phospho-NF-κB p65 (3033, CST, USA), anti-NF-κB p65 (8242, CST, USA), anti-p38 (9212, CST, USA), anti-phospho-p38 (9211, CST, USA), anti-ERK (9102, CST, USA), anti-phospho-ERK (4370, CST, USA), anti-JNK (9252, CST, USA), anti-phospho-JNK (92551, CST, USA), anti-β-actin (60009-1-Ig, Proteintech, China), anti-Lamin-B1 (12987-1-AP, Proteintech, USA), and anti-Bax (2772, CST, USA). Subsequently, the membrane was incubated with anti-mouse/anti-rabbit secondary antibody for 2 h. Finally, the protein signal was visualized using an enhanced chemiluminescence system.

Plasmids and Transfection

PDCD4-shRNA and Neo-shNC (negative control) plasmids were purchased from China Gene Pharma. We used Lipofectamine3000 reagent to transiently transfect the plasmids into BV2 cells or HT22 cells in accordance with the manufacturer's instructions.

Table 2

The target sequences of PDCD4-shRNA.

	target sequences
sh-PDCD4#1	5'-GGAAGTGAAGCGGTTAGAAGT-3'
sh-PDCD4#2	5'-GGAAGAGGTGGATGTGAAAGA-3'
sh-PDCD4#3	5'-GGGACGGTGATGAGCACAAAT-3'
sh-PDCD4#4	5'-GCTGCTCTGGATAAGGCTACT-3'

Measurement of intracellular reactive oxygen species production

Intracellular reactive oxygen species (ROS) levels were examined by the DCFH-DA method in accordance with the manufacturer’s instruction. Briefly, BV2 cells were transfected with the plasmid for 48 h, stimulated with LPS (100 ng/mL) for 12 h, washed with PBS, and treated with serum-free medium containing DCFH-DA (S30033S, Beyotime, China) in the incubator for 20 min. Next, the cells were washed

with serum-free cell culture medium for three times and observed using a fluorescence microscope (ECLIPSE Ti-E, Nikon, Japan).

Nuclear and cytoplasmic extraction experiment

An NE-PER Nuclear Protein-Cytoplasmic Protein Extraction Kit (78833, Thermo Fisher, USA) was used to separate the subcellular fractions in accordance with the manufacturer's instructions. Briefly, BV2 cells were washed with ice-cold PBS and lysed in CER I working reagent protease containing protease inhibitors for 10 min on ice. After adding CER I working reagent, cytosolic protein isolation was performed by centrifuging the supernatant. Then, the addition of the NER working reagent to the cell pellet caused the release of the cytoplasmic content. The protein concentration was quantified using the BCA Protein Assay Kit (23225, ThermoFish, USA).

Cell Viability Assay

MTT analysis was used to evaluate the viability of HT22 cells after exposure to different concentrations of H_2O_2. In short, HT22 cells were seeded on a 96-well microtiter plate at a density of 0.6×104 cells/well. After treatment with different concentrations of H_2O_2, the MTT working solution (5 mg/mL) was added to each well and incubated for 4 h at 37°C. Then, DMSO was added to dissolve formazan crystals. Finally, the MTT product was calculated with a microplate reader (Synergy H1, BioTek, USA) and analyzed by GraphPad 8.4 system.

Statistical Analysis

Statistical analysis was conducted using GraphPad Prism 8.4.3 software. The data were calculated as mean ± standard deviation (SD). The differences between the groups were detected by t tests and followed by Tukey's post hoc multiple comparison tests. The P values below 0.05 were considered statistically significant.

Results

PDCD4 expression was upregulated in the inflamed mice cerebral cortex following LPS intraperitoneal injection

To explore the expression and function of PDCD4 in neuroinflammation, we established the classical neuroinflammation model induced by LPS intraperitoneal injection in mice[6]. The mRNA expression levels of proinflammatory genes (TNF-α, IL-1β, IL-6, and inducible nitric oxide synthase (iNOS)) in the cerebral cortex of mice were significantly upregulated after LPS stimulation, reaching their peak values around the third day (Fig. 1A). Western blot confirmed the increased levels of proinflammatory protein

iNOS and proapoptotic protein cleaved-parp in the inflamed cerebral cortex (Fig. 1B). All of these results indicated that LPS successfully induced CNS inflammation and neuronal injury in mice. Next, we used western blot to examine the changes in PDCD4 expression in the brain tissue (Fig. 1B). The PDCD4 level was lower in the cerebral cortex of the saline-injected control group, gradually increased 12 h after the LPS injection, reached the peak on day 1, and then decreased back to the basal level by day 7. Immunohistochemical staining further clarified the expression and distribution of PDCD4. Compared with the control group, the number and intensity of PDCD4-positive cells in the cerebral cortex increased significantly one day after the LPS administration, which was consistent with the results of the western blot analysis (Fig. 1C)

Elevated PDCD4 expression was associated with neuronal apoptosis and microglial activation in the inflamed mice brainn

To further determine the cell types expressing PDCD4 protein, we employed double immunofluorescence staining and investigated the possible co-localization of PDCD4 with different cell markers, including NeuN (neuronal marker), GFAP (astrocytic marker), and Iba1 (microglial marker) in the mouse brain. As shown in Fig. 2, an elevated PDCD4 expression level was mainly observed in NeuN-positive neurons and Iba1-positive microglia in the mouse cerebral cortex one day after the LPS administration (Fig. 2A, B). No apparent co-localization was detected between PDCD4 and GFAP (the astrocyte marker) (Fig. 2C). Double immunofluorescence staining demonstrated a clear co-localization of PDCD4 with the inflammatory marker iNOS and cellular apoptotic marker cleaved-caspase3 in the LPS-injected group (Fig. 2D and E). These results indicated that PDCD4 may be a hub molecule that simultaneously participates in microglial inflammatory activation and neuronal apoptosis in the LPS-triggered neuroinflammation.

Increased PDCD4 expression in the LPS-activated BV2 microglia cells

To further analyze the contribution of PDCD4 to neuroinflammation, we established an in vitro microglial activation model. LPS (100 ng/mL) was used to stimulate BV2 microglia cells. Real-time PCR assay demonstrated a time-dependent increase in proinflammatory marker genes (iNOS, TNF-α, and IL-1β) in BV2 cells following the LPS administration (Fig. 3A). Western blot analysis confirmed the elevation of the inflammatory proteins (iNOS and IL-1β), with the maximum levels achieved at 12 h (Fig. 3B). In line with the in vivo results, microglial PDCD4 expression was significantly induced by LPS stimulation, reached the peak at 12 h, and declined thereafter (Fig. 3B). These data further indicated that PDCD4 was closely associated with microglial inflammatory activation.

PDCD4 knockdown suppressed the expression of proinflammatory factors and ROS production in microglia

To explore the potential function of PDCD4 in the inflammatory activation of microglia, we silenced PDCD4 expression in BV2 cells by RNA interference (RNAi) and confirmed the interference efficiency by western blot (Fig. 4A). Since sh-PDCD4#4 exerted the best silencing effect, it was employed in the subsequent experiments. Western blot revealed that LPS triggered the proinflammatory iNOS expression in BV2 cells (Fig. 4B). RT-PCR also showed the elevated transcription level of proinflammatory genes, such as TNF-α, IL-1β, and iNOS (Fig. 4C). Compared with the scrambled control shRNA group (sh-Ctrl), knocking down PDCD4 significantly attenuated the expression of the LPS-induced proinflammatory factors in BV2 microglia (Fig. 4B and C). Additionally, silencing PDCD4 largely suppressed the LPS-induced ROS production in BV2 cells (Fig. 4D). Thus, despite conflicting data in the previous reports regarding the function of PDCD4 in inflammation, our data demonstrated that PDCD4 facilitates the LPS-induced microglial inflammatory activation.

Silencing PDCD4 inhibited the MAPK-NF-κB proinflammatory signaling pathway in the LPS-treated microglia

Next, we investigated the possible downstream signaling pathway through which PDCD4 regulates microglial activation. Western blot analysis showed that LPS sharply induced the phosphorylation of JNK (p-JNK), p38 (p-p38), and ERK (p-ERK) in BV2 cells, indicating the activation of the classical proinflammatory MAPK signaling pathway (Fig. 5A). Moreover, apparent phosphorylation of NF-κB p65 (p-p65) and its nuclear transportation represented the activation of the pivotal proinflammatory transcription factor (Fig. 5A and B). Compared with the control group, silencing PDCD4 significantly inhibited the LPS-induced phosphorylation of all three MAPK branches (JNK, p38, and ERK) in BV2 microglia (Fig. 5A). Moreover, knocking down PDCD4 suppressed the NF-κB p65 phosphorylation and its nuclear accumulation in the LPS-treated cells (Fig. 5A and B). Our data suggested that PDCD4 promoted the LPS-induced microglial activation by upregulating the classical MAPK-NF-κB proinflammatory signaling pathway.

LPS required the MAPK-NF-κB signaling pathway to elevate PDCD4 expression in microglia

To examine the possible mechanism regulating PDCD4 expression in microglia, we utilized the specific inhibitors of MAPKs or NF-κB to pre-treat BV2 cells followed before LPS administration (Fig. 6A). Western blot showed that all of the MAPK inhibitors (SB20358 for p38, PD98059 for ERK, and SP600125 for JNK) prevented the LPS-induced iNOS expression (Fig. 6B), proving their anti-inflammatory function.

Interestingly, inhibition of the MAPK signaling pathways significantly reversed the LPS-induced elevated PDCD4 protein expression in BV2 cells (Fig. 6B). Moreover, specific inhibition of NF-κB activity by Bay11-7082 significantly attenuated the LPS-triggered expression of PDCD4 and iNOS (Fig. 6B). Taken together, our results implied that LPS required the MAPK-NF-κB signaling pathway to elevate PDCD4 expression in microglia, indicating the presence of a positive feedback loop to promote neuroinflammation.

PDCD4 contributed to the oxidative damage of neurons

It is well understood that the reactive oxygen species released by activated microglia can greatly damage the neighboring neurons. Since our results from the in vivo experiments indicated the co-localization of PDCD4 with NeuN and cleaved-caspase 3 in the inflamed mouse brain, we next evaluated the potential role of PDCD4 in the neuronal oxidative damage model in vitro. Different concentrations of hydrogen peroxide (H_2O_2) were employed to stimulate the mouse hippocampal neuron cell line HT22. The MTT assay demonstrated a concentration-dependent decrease in cell viability (Fig. 7A). Since 400 μM H_2O_2 treatment for 24 h resulted in a moderate decline in cell viability (about 40%) in HT22 cells (Fig. 7A), we chose this concentration for the subsequent experiments. Western blot revealed a time-dependent induction of the typical proapoptotic protein BAX in HT22 cells by H_2O_2 administration (Fig. 7B). A time-dependent continuous elevation in PDCD4 protein level was observed in this neuronal oxidative damage model (Fig. 7B). More importantly, knocking down PDCD4 by shRNA significantly inhibited the expression of the proapoptotic factor BAX in HT22 cells (Fig. 7C). These data indicated that PDCD4 played a pivotal role in promoting reactive oxygen-related neuronal damage and acted as a shared regulatory molecule for both microglial activation and neuronal injury during neuroinflammation.

Discussion

Neuroinflammation, the immune response in the nervous system, normally plays a protective role to promote neuronal repair and regeneration. However, persistent neuroinflammation disturbs the brain homeostasis and causes progressive neuron loss and dysfunction, which is a common pathological mechanism for CNS diseases[1][7]. Identifying a shared hub molecule which is simultaneously involved in both neuroinflammation and neuronal apoptosis would be of great significance for the in-depth understanding of the pathogenesis of neurological diseases. In this study, we demonstrated that the tumor suppressor PDCD4 acts as a common molecule that simultaneously promotes inflammatory activation of microglia and oxidative stress-mediated apoptosis of neurons. Moreover, we proved the existence of a positive feedback loop of PDCD4–MAPK–NF-κB that accelerates the LPS-induced neuroinflammation; indeed, this loop might become a novel therapeutic target for neuroinflammatory diseases.

PDCD4 (programmed cell death protein 4) was originally cloned as a novel apoptosis-inducible gene in the experimental apoptosis models[29]. It is highly conserved during evolution and ubiquitously expressed in normal tissues and organs[8]. Decreased PDCD4 expression was observed in various

tumors, such as lung cancer, colorectal cancer, breast cancer, hepatocellular carcinoma, and glioblastoma[19][30][31]. Some proapoptotic drugs (such as ionomycin), antineoplastic drugs (such as retinoic acid receptor agonist), or cytokines (including IL-12 and TGF-β1) can stimulate PDCD4 expression[18][19] Considering its pivotal functions in the regulation of cellular apoptosis, the potential roles of PDCD4 during neuronal injury have gradually attracted research attention. Chronic restraint stress increased PDCD4 expression in mice hippocampus by decreasing the mTORC1-mediated proteasomes degradation[32]. Elevated PDCD4 expression was observed in the rat spinal cord injury model[33], the chronic sciatic nerve injury (CCI)-induced rat neuropathic pain model[34], the oxygen-glucose deprivation/reoxygenation (OGDR) injury model of rat hippocampal neurons[35], and the ischemia and reperfusion (I/R)-induced neuronal lesion model in mouse retina [25]. The available studies have indicated that PDCD4 may be extensively involved in neuronal damage. However, to the best of our knowledge, the expression and biological function of PDCD4 during LPS-induced neuroinflammation, especially its role in the interaction between neuroinflammation and neuronal injury, have not been systematically studied. In this study, we detected an inducible expression of PDCD4 in the mouse neuroinflammation model by LPS intraperitoneal injection; the expression peaked after one day and regressed to the baseline on day 7. Immunohistochemistry staining revealed the presence of PDCD4 both in injured neurons and activated microglia in the inflamed mouse brain (Fig. 1 and 2). A similar change in PDCD4 expression was observed in the LPS-induced BV2 microglial inflammatory activation model (Fig. 3). These data indicate a potential involvement of PDCD4 during the LPS-induced neuroinflammation and neuronal injury in mouse brain.

Although previous studies implied a close association between PDCD4 and inflammatory diseases, the conflicting experimental data made it difficult to determine its exact biological function and mechanisms[8]. There is some evidence that PDCD4 is a proinflammatory molecule. For example, PDCD4 deficiency significantly inhibited the JNK phosphorylation, NF-κB activation, and IL-6 production in mice macrophages[23], and PDCD4-deficient mice were protected from LPS-induced death[20]. PDCD4 overexpression exaggerated the apoptosis and proinflammatory cytokine production in toxin-treated intestinal porcine epithelial cells, thereby aggravating cellular damage[36]. However, other results suggested an anti-inflammatory role for PDCD4. For instance, PDCD4 deficiency aggravated the experimental colitis and colitis-associated colorectal carcinoma (CRC) in mice by accelerating the typical proinflammatory IL-6/STAT3 pathway[24]. In the LPS or D-galactosamine (D-GalN)-induced acute liver injury model, compared with the wild-type mice, PDCD4-deficient mice presented more necrotic and apoptotic hepatocytes, inflammatory cells infiltration, inflammatory cytokine (IL-6 and TNF-α) release, and liver internal hemorrhage [37]. In the current study, to identify the biological function of PDCD4 in neuroinflammation, we silenced its expression by shRNA; our results showed that knocking down PDCD4 significantly attenuated the expression of proinflammatory cytokines (IL-1β and TNFα), iNOS, and ROS production in microglia (Fig. 4). More importantly, silencing PDCD4 inhibited the phosphorylation and activation of all three substreams of the MAPK signaling (p38, ERK, and JNK) and prevented the phosphorylation and nuclear transportation of NF-κB p65 (Fig. 5). Taken together, our data demonstrated

that PDCD4 facilitates the LPS-induced microglial inflammatory activation by promoting the pivotal MAPK/NF-κB signaling pathway.

The mechanisms regulating PDCD4 expression during inflammation remain unclear, but PDCD4 involvement in oncology may provide some clues. Namely, PDCD4 expression is reportedly regulated at different levels[18][19]. The epigenetic silencing by promoter methylation and some transcription factors such as FOXO and v-myb directly regulate the PDCD4 expression at the transcriptional level[18][19]. SRSF3 modulates PDCD4 expression by inhibiting the alternative splicing and nuclear export of Pdcd4 mRNA at the post-transcriptional level[8, 9]. Some non-coding RNAs, typically miR-21 and lncRNA MALAT1, bind and form sponging to target PDCD4 expression directly at the translational level[18][19]. Moreover, protein–protein interactions (such as BCL6–PDCD4), phosphorylation, and ubiquitination modifications reportedly regulate PDCD4 activity, nuclear transfer, and protein degradation at the post-translational level[18][19]. In this study, utilizing the specific chemical inhibitors to pre-treat BV2 cells, we found that specifically blocking the MAPKs (p38, ERK, or JNK) or NF-κB activation significantly suppressed the LPS-induced PDCD4 protein expression in BV2 cells (Fig. 6). Our results indicated that LPS requires the MAPK-NF-κB signaling pathway to stimulate PDCD4 expression, which suggests that a PDCD4–MAPK–NF-κB positive feedback loop is formed to drive the microglial inflammatory activation. Further investigations are needed to explore the exact underlying mechanisms.

PDCD4 was first discovered as an apoptosis-related gene[29], and its involvement in cellular apoptosis has been extensively documented. In Huh7 hepatoma cells, PDCD4 overexpression elevated the expression of BAX, the proapoptotic member of Bcl2 protein family; moreover, it promoted the release of cytochrome C from mitochondria and activation of caspases 8, 9, and 3, thereby accelerating cellular apoptosis[38]. PDCD4 specifically binds to the internal ribosome entry site (IRES) elements of both the XIAP and Bcl-x(L) messenger RNAs, represses the translation of these anti-apoptotic proteins by inhibiting the formation of the 48S translation initiation complex, and thus promotes apoptosis[39]. A recent study implied that miR-183-5p may directly target PDCD4 and RIPK3 to protect neurons from apoptosis and necroptosis during amyotrophic lateral sclerosis (ALS)[40]. MiR-21 derived from the exosomes of mesenchymal stem cells (MSCs) suppressed neuronal death via inhibiting PDCD4 and PTEN signaling pathways[17]. Moreover, miR-340-5p performed neuroprotective function by targeting PDCD4 and then activating the PI3K/Akt pathway in rat hippocampal neurons exposed to OGDR injury[35]. LncRNA-H19 facilitated PDCD4 expression via sponging miR-21 and regulated the ischemia and reperfusion (I/R)-induced sterile inflammation and neuronal lesion in mice retinas[25]. Oxidative stress, defined as excess production of reactive oxygen species (ROS), is a typical feature of neuroinflammation, and directly leads to subsequent neuronal damage[4]. In the present study, a persistent elevation of PDCD4 expression was detected in the H_2O_2-induced neuron oxidative damage model. Knocking down PDCD4 significantly inhibited the expression of the proapoptotic protein BAX, suggesting the proapoptotic activity of PDCD4 in the oxidative stress-induced neuronal injury (Fig. 7).

In summary, we found that PDCD4 can serve as a hub regulatory molecule that promotes both microglial inflammatory activation and oxidative stress-induced neuronal apoptosis within CNS. Moreover, we

proved that PDCD4/MAPKs/NF-κB can form a positive feedback loop to exaggerate the vicious cycle of neuroinflammation and neuronal injury, which might become the potential therapeutic target for the treatment of neuroinflammatory diseases.

Declarations

Funding

This work was supported by Scientific Research Project of Health Commission of Jiangsu Province (H2018035, LGY2017042); Scientific Research Project of "333 Project" in Jiangsu Province (BRA2018224); Nantong Science and Technology Project (JC2019031 and JCZ20078); the "Top Six Types of "Financial Assistance of Jiangsu Province Grant (2019-WSW-199); Nantong University School-level Fund Project (2019JZ005).

Conflicts of interest

The authors declare that they have no conflict of interest.

Availability of Data and Material

All data generated and analyzed during this study are included in this published article.

Code Availability

Not applicable.

Authors' Contributions

Dongmei Zhang, Hongjian Lu, Chengwei Duan, Xiangyang Zhu, and Yi Zhang designed the research; Quan Chen performed all the experiments; Quan Chen and Mengmeng Li constructed the animal model; Chengwei Duan and Mengmeng Li assisted with the experiments; Hongjian Lu, Chengwei Duan, Xiangyang Zhu, Yi Zhang and Dongmei Zhang analyzed and interpreted the data; Quan Chen, Hongjian Lu and Dongmei Zhang wrote and revised the manuscript; and all authors approved the final version of the manuscript.

Ethics Approval

All animal experiments were performed according to the protocol approved by the Animal Experimental Ethics Committee of Nantong University.

Consent to Participate

Not applicable.

Consent for Publication

Not applicable.

References

1. Xu, Y., M. Z. Jin, Z. Y. Yang, and W. L. Jin. 2021. Microglia in neurodegenerative diseases. *Neural Regen Res* 16 (2): 270–280. doi:10.4103/1673-5374.290881.
2. Lian, L., Y. Zhang, L. Liu, L. Yang, Y. Cai, J. Zhang, and S. Xu. 2020. Neuroinflammation in Ischemic Stroke: Focus on MicroRNA-mediated Polarization of Microglia. *Front Mol Neurosci* 13: 612439. doi:10.3389/fnmol.2020.612439.
3. Zhang, W., T. Tian, S. X. Gong, W. Q. Huang, Q. Y. Zhou, A. P. Wang, and Y. Tian. 2021. Microglia-associated neuroinflammation is a potential therapeutic target for ischemic stroke. *Neural Regen Res* 16 (1): 6–11. doi:10.4103/1673-5374.286954.
4. Schirmer, Lucas, Dorothy P Schafer, Theresa Bartels, David H Rowitch, and A Calabresi Peter. 2021. Diversity and Function of Glial Cell Types in Multiple Sclerosis. *Trends in Immunology*. doi:10.1016/j.it.2021.01.005.
5. Harms, Ashley S, A. Sara, Ferreira, and Marina Romero-Ramos. 2021. Periphery and brain, innate and adaptive immunity in Parkinson's disease. Acta Neuropathologica:1–19.doi:10.1007/s00401-021-02268-5.
6. Leng, Fangda, and Paul Edison. 2020. Neuroinflammation and microglial activation in Alzheimer disease: where do we go from here? Nature Reviews Neurology:1–16.doi:10.1038/s41582-020-00435-y.
7. Wake, Hiroaki, Hiroshi Horiuchi, Daisuke Kato, and Andrew J Moorhouse, and Junichi Nabekura. 2019. Physiological Implications of Microglia–Synapse Interactions. *Microglia*:69–80.doi: 10.1007/978-1-4939-9658-2-6.
8. Chen, Zhihong, and D Trapp Bruce. 2016. Microglia and neuroprotection. *Journal of neurochemistry* 136: 10–17. doi:10.1111/jnc.13062.
9. Conti, Pio, Dorina Lauritano, Alessandro Caraffa, Carla Enrica Gallenga, K. Spiros, Gianpaolo Kritas, and Ronconi, and Stefano Martinotti. 2020. Microglia and mast cells generate proinflammatory cytokines in the brain and worsen inflammatory state: suppressor effect of IL-37. European journal of pharmacology 875:173035.doi: 10.1016/j.ejphar.2020.173035.
10. Barichello, Tatiana, Lutiana R Simoes, Joao Quevedo, and Y. Xiang, and Zhang. 2019. Microglial activation and psychotic disorders: evidence from pre-clinical and clinical studies.

*Neuroinflammation and Schizophreni*a:161–205.doi: 10.1007/7854_2018_81.

11. Bagheri-Mohammadi, Saeid. 2021. Microglia in Alzheimer's Disease: The Role of Stem Cell-Microglia Interaction in Brain Homeostasis. *Neurochemical Research* 46 (4): 1–8. doi:10.1007/s11064-020-03162-4.
12. Simpson, Dominic SA, and L Oliver Peter. 2020. ROS generation in microglia: Understanding oxidative stress and inflammation in neurodegenerative disease. *Antioxidants* 9 (8): 743. doi:10.3390/antiox9080743.
13. Hickman, Suzanne, Saef Izzy, Pritha Sen, and Liza Morsett, and Joseph El Khoury. 2018. Microglia in neurodegeneration. Nature Neuroscience 21 (10):1359–1369.doi:10.1038/s41593-018-0242-x.
14. Zhang, D., L. Sun, H. Zhu, L. Wang, W. Wu, J. Xie, and J. Gu. 2012. Microglial LOX-1 reacts with extracellular HSP60 to bridge neuroinflammation and neurotoxicity. *Neurochem Int* 61 (7): 1021–1035. doi:10.1016/j.neuint.2012.07.019.
15. Ge, X., D. M. Zhang, M. M. Li, Y. Zhang, X. Y. Zhu, Y. Zhou, X. Peng, and A. G. Shen. 2019. Microglial LOX-1/MAPKs/NF-kappaB positive loop promotes the vicious cycle of neuroinflammation and neural injury. *Int Immunopharmacol* 70: 187–200. doi:10.1016/j.intimp.2019.02.013.
16. Li, M., D. Zhang, X. Ge, X. Zhu, Y. Zhou, Y. Zhang, X. Peng, and A. Shen. 2019. TRAF6-p38/JNK-ATF2 axis promotes microglial inflammatory activation. *Exp Cell Res* 376 (2): 133–148. doi:10.1016/j.yexcr.2019.02.005.
17. Yoshinaga, H., S. Matsuhashi, C. Fujiyama, and Z. Masaki. 1999. Novel human PDCD4 (H731) gene expressed in proliferative cells is expressed in the small duct epithelial cells of the breast as revealed by an anti-H731 antibody. *Pathol Int* 49 (12): 1067–1077. doi:10.1046/j.1440-1827.1999.00995.x.
18. Lu, K., Q. Chen, M. Li, L. He, F. Riaz, T. Zhang, and D. Li. 2020. Programmed cell death factor 4 (PDCD4), a novel therapy target for metabolic diseases besides cancer. *Free Radic Biol Med* 159: 150–163. doi:10.1016/j.freeradbiomed.2020.06.016.
19. Matsuhashi, S., M. Manirujjaman, H. Hamajima, and I. Ozaki. 2019. Control Mechanisms of the Tumor Suppressor PDCD4: Expression and Functions. Int J Mol Sci 20 (9). doi:10.3390/ijms20092304.
20. Long, J., Y. Yin, H. Guo, S. Li, Y. Sun, C. Zeng, and W. Zhu. 2019. The mechanisms and clinical significance of PDCD4 in colorectal cancer. *Gene* 680: 59–64. doi:10.1016/j.gene.2018.09.034.
21. Zhao, Mengxiang, Nisha Zhu, Fengyao Hao, and Yuxian Song, and Liang Ding. 2019. The Regulatory Role of Non-coding RNAs on Programmed Cell Death Four in Inflammation and Cancer. *Frontiers in Oncology* 9: 919. doi:10.3389/fonc.2019.00919.
22. Wang, Q., Z. Dong, X. Liu, X. Song, Q. Song, Q. Shang, Y. Jiang, C. Guo, and L. Zhang. 2013. Programmed cell death-4 deficiency prevents diet-induced obesity, adipose tissue inflammation, and insulin resistance. *Diabetes* 62 (12): 4132–4143. doi:10.2337/db13-0097.
23. Sheedy, F. J., E. Palsson-McDermott, E. J. Hennessy, C. Martin, J. J. O'Leary, Q. Ruan, D. S. Johnson, and Y. Chen, and L. A. O'Neill. 2010. Negative regulation of TLR4 via targeting of the proinflammatory

tumor suppressor PDCD4 by the microRNA miR-21. Nat Immunol 11 (2):141–147. doi:10.1038/ni.1828.

24. Wang, L., M. Zhao, C. Guo, G. Wang, F. Zhu, J. Wang, and X. Wang, et al. 2016. PDCD4 Deficiency Aggravated Colitis and Colitis-associated Colorectal Cancer Via Promoting IL-6/STAT3 Pathway in Mice. *Inflamm Bowel Dis* 22 (5): 1107–1118. doi:10.1097/MIB.0000000000000729.
25. Wan, P., W. Su, Y. Zhang, Z. Li, C. Deng, J. Li, N. Jiang, S. Huang, E. Long, and Y. Zhuo. 2020. LncRNA H19 initiates microglial pyroptosis and neuronal death in retinal ischemia/reperfusion injury. *Cell Death Differ* 27 (1): 176–191. doi:10.1038/s41418-019-0351-4.
26. Salazar, Alexander, Bryan L Gonzalez-Rivera, Laney Redus, Jennifer M Parrott, and Jason C O'Connor. 2012. Indoleamine 2, 3-dioxygenase mediates anhedonia and anxiety-like behaviors caused by peripheral lipopolysaccharide immune challenge. *Hormones and behavior* 62 (3): 202–209. doi:10.1016/j.yhbeh.2012.03.010.
27. Zhang, Yu, Xiaojuan Liu, Huaqing Xue, Xiaorong Liu, Aihua Dai, Yan Song, Kaifu Ke, and Maohong Cao. 2016. Upregulation of PRDM5 Is Associated with Astrocyte Proliferation and Neuronal Apoptosis Caused by Lipopolysaccharide. *Journal of Molecular Neuroscience* 59 (1): 146–157. doi:10.1007/s12031-016-0744-5.
28. Ross, Erika K, N. Aimee, Heather M Winter, A. Wilkins, Whitney, Nathan Sumner, David Duval, Patterson, and A Linseman Daniel. 2014. A cystine-rich whey supplement (Immunocal®) delays disease onset and prevents spinal cord glutathione depletion in the hSOD1G93A mouse model of amyotrophic lateral sclerosis. *Antioxidants* 3 (4): 843–865. doi:10.1155/2017/3103272.
29. Shibahara, K., M. Asano, Y. Ishida, T. Aoki, T. Koike, and T. Honjo. 1995. Isolation of a novel mouse gene MA-3 that is induced upon programmed cell death. *Gene* 166 (2): 297–301. doi:10.1016/0378-1119(95)00607-9.
30. Long, J., Y. Yin, H. Guo, S. Li, Y. Sun, C. Zeng, and W. Zhu. 2019. The mechanisms and clinical significance of PDCD4 in colorectal cancer. *Gene* 680: 59–64. doi:10.1016/j.gene.2018.09.034.
31. Li, C., Y. Chen, X. Chen, Q. Wei, R. Ou, X. Gu, B. Cao, and H. Shang. 2020. MicroRNA-183-5p is stress-inducible and protects neurons against cell death in amyotrophic lateral sclerosis. *J Cell Mol Med* 24 (15): 8614–8622. doi:10.1111/jcmm.15490.
32. Li, Y., Y. Jia, D. Wang, X. Zhuang, Y. Li, C. Guo, and H. Chu, et al. 2020. Programmed cell death 4 as an endogenous suppressor of BDNF translation is involved in stress-induced depression. *Mol Psychiatry*. doi:10.1038/s41380-020-0692-x.
33. Kang, J., Z. Li, Z. Zhi, S. Wang, and G. Xu. 2019. MiR-21 derived from the exosomes of MSCs regulates the death and differentiation of neurons in patients with spinal cord injury. *Gene Ther* 26 (12): 491–503. doi:10.1038/s41434-019-0101-8.
34. Peng, C., C. Zhang, Z. Su, and D. Lin. 2019. DGCR5 attenuates neuropathic pain through sponging miR-330-3p and regulating PDCD4 in CCI rat models. *J Cell Physiol* 234 (5): 7292–7300. doi:10.1002/jcp.27487.

35. Zheng, Yake, Peng Zhao, Yajun Lian, Shuang Li, and Lihao Li. 2019. MiR-340-5p alleviates oxygen-glucose deprivation/reoxygenation-induced neuronal injury via PI3K/Akt activation by targeting PDCD4. *Neurochemistry International* 134: 104650. doi:10.1016/j.neuint.
36. Gao, X., X. Huang, Q. Yang, S. Zhang, Z. Yan, R. Luo, P. Wang, W. Wang, K. Xie, and S. Gun. 2021. MicroRNA-21-5p targets PDCD4 to modulate apoptosis and inflammatory response to Clostridium perfringens beta2 toxin infection in IPEC-J2 cells. *Dev Comp Immunol* 114: 103849. doi:10.1016/j.dci.2020.103849.
37. Wang, X., L. Zhang, Z. Wei, X. Zhang, Q. Gao, Y. Ma, and X. Liu, et al. 2013. The inhibitory action of PDCD4 in lipopolysaccharide/D-galactosamine-induced acute liver injury. *Lab Invest* 93 (3): 291–302. doi:10.1038/labinvest.2012.174.
38. Zhang, H., I. Ozaki, T. Mizuta, H. Hamajima, T. Yasutake, Y. Eguchi, H. Ideguchi, K. Yamamoto, and S. Matsuhashi. 2006. Involvement of programmed cell death 4 in transforming growth factor-beta1-induced apoptosis in human hepatocellular carcinoma. *Oncogene* 25 (45): 6101–6112. doi:10.1038/sj.onc.1209634.
39. Liwak, U., N. Thakor, L. E. Jordan, R. Roy, S. M. Lewis, O. E. Pardo, M. Seckl, and M. Holcik. 2012. Tumor suppressor PDCD4 represses internal ribosome entry site-mediated translation of antiapoptotic proteins and is regulated by S6 kinase 2. *Mol Cell Biol* 32 (10): 1818–1829. doi:10.1128/MCB.06317-11.
40. Li, C., Y. Chen, X. Chen, Q. Wei, R. Ou, X. Gu, B. Cao, and H. Shang. 2020. MicroRNA-183-5p is stress-inducible and protects neurons against cell death in amyotrophic lateral sclerosis. *J Cell Mol Med* 24 (15): 8614–8622. doi:10.1111/jcmm.15490.

Figures

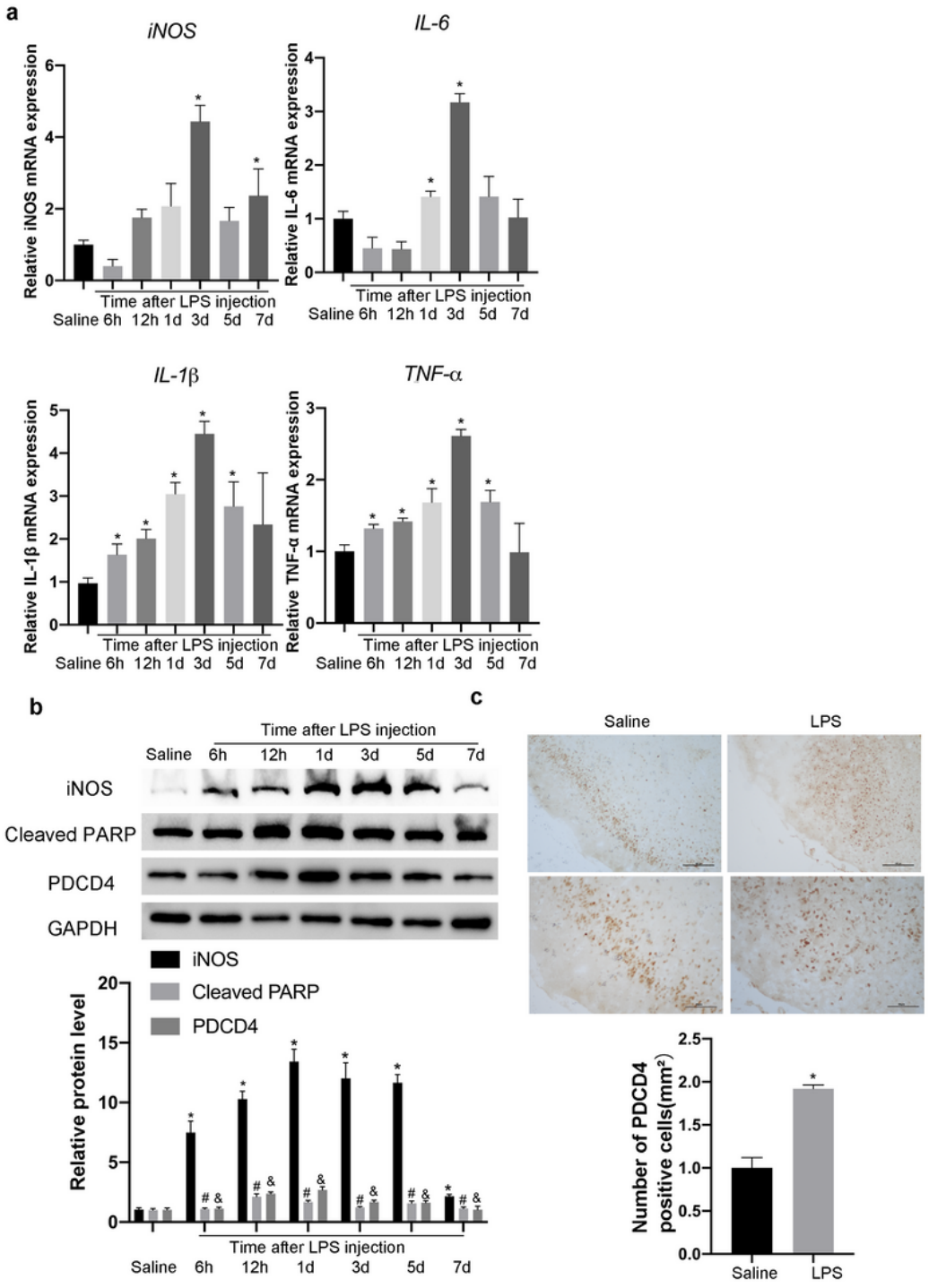

Figure 1

Elevated PDCD4 expression in the inflamed mice cerebral cortex following LPS intraperitoneal injection. (A) The CNS inflammation model was established by LPS intraperitoneal injection in mice. RT-PCR detected the mRNA levels of TNF-α, IL-1β, IL-6, and iNOS in the cerebral cortex of mice following the LPS treatment. (B) Western blot was used to detect the expression of iNOS, Cleaved-PARP, and PDCD4 in the cerebral cortex. (C) Immunohistochemical staining detected PDCD4 expression and distribution in the

sham operation group (Saline) and the LPS group one day after the injection. (*p <0.05, #p<0.05, &p<0.05).

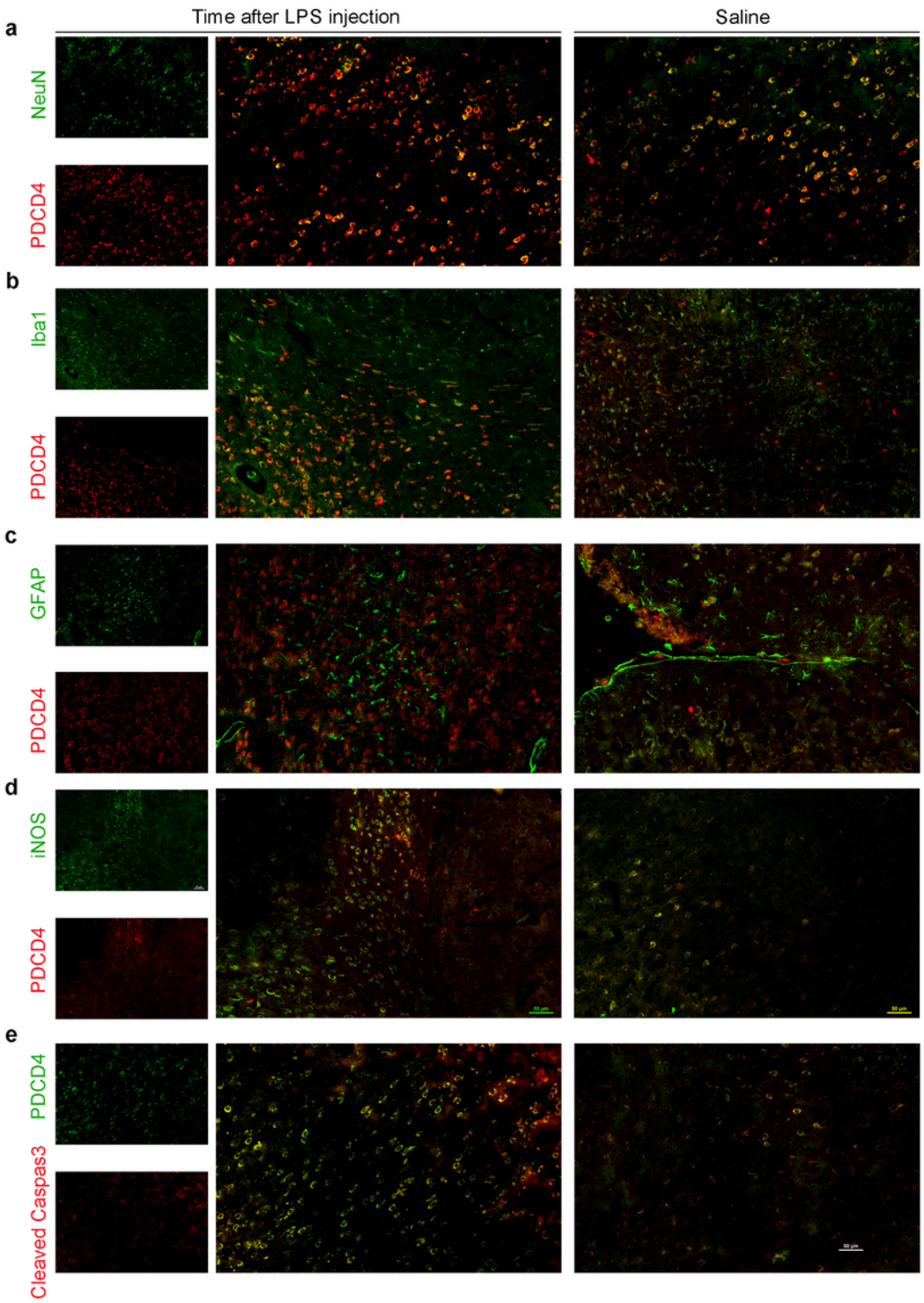

Figure 2

Immunofluorescence staining of PDCD4 and different phenotype-specific markers in the inflamed mouse cerebral cortex. The sections of the mouse cerebral cortex on the first day after the LPS or saline injection were labeled with PDCD4 and different cell markers, including the neuron marker (A, NeuN, green), the

microglia marker (B, Iba1, green), the astrocyte marker (C, GFAP, green), the inflammation-related proteins (D, iNOS, green), or the proapoptotic protein (E, Cleaved-Caspase3, red). The scale bar is 50 μm.

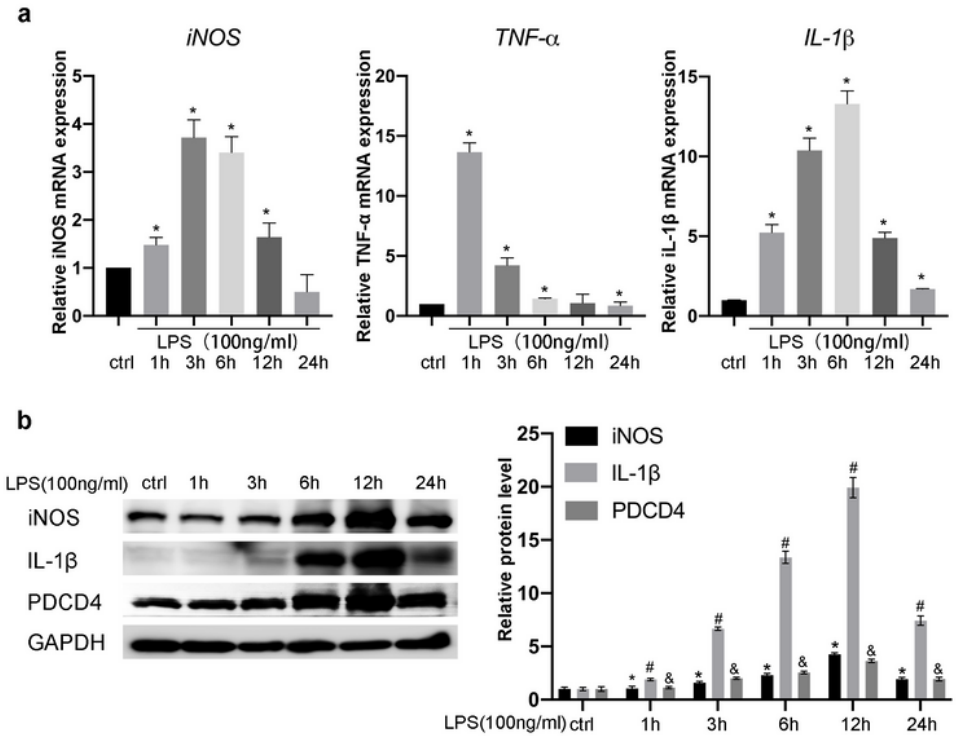

Figure 3

Upregulation of PDCD4 in LPS-activated BV2 microglial cells. BV2 microglial cells were treated with LPS (100 ng/mL) for different periods (0 h, 1 h, 3 h, 6 h, 12 h, or 24 h). (A) RT-PCR detection of iNOS, TNF-α,

and IL-1β mRNA expression. (B) Western blot analysis of the levels of PDCD4, iNOS, and iL-1β protein. (*p<0.05, #p<0.05).

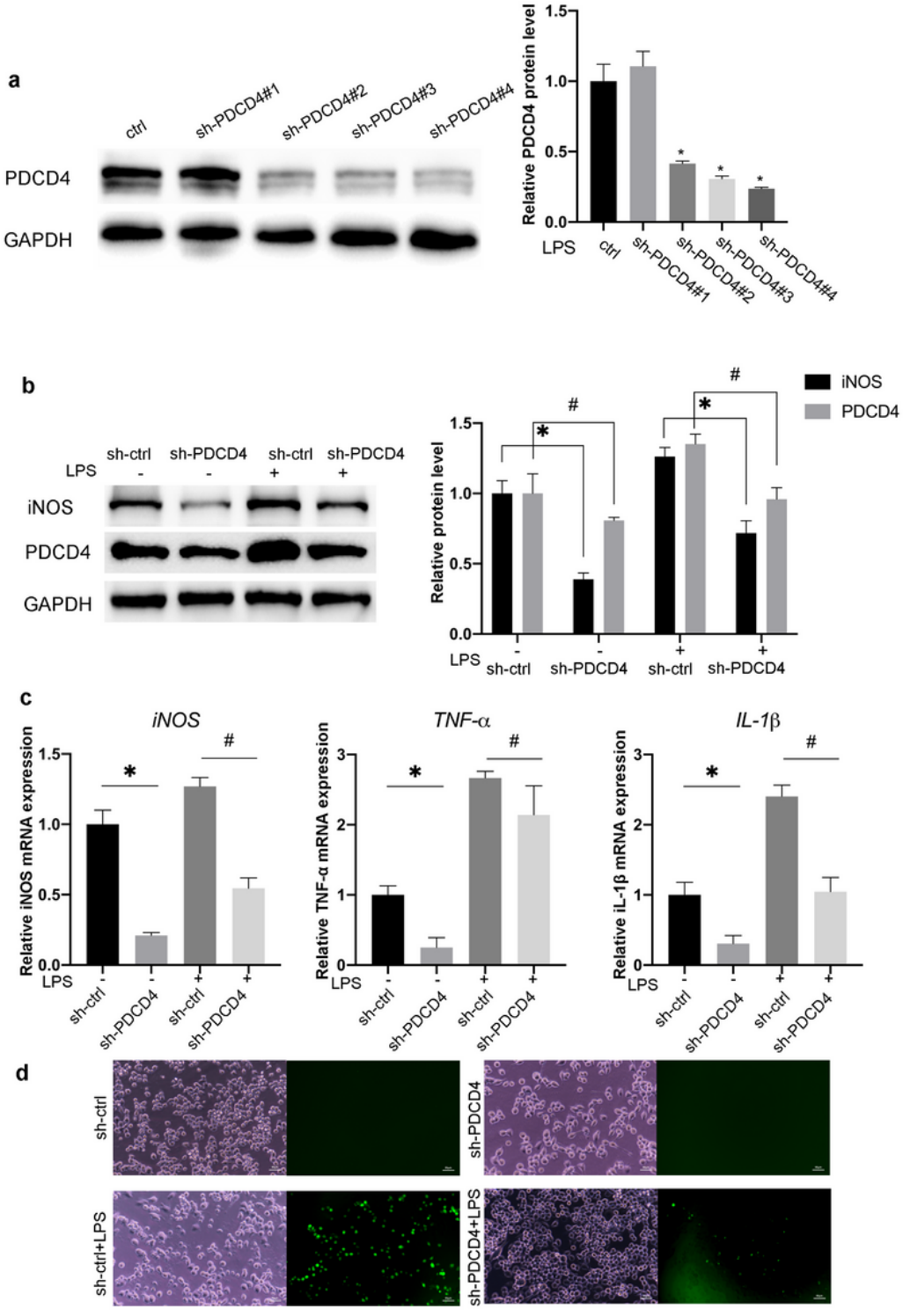

Figure 4

PDCD4 knockdown reduced the expression of proinflammatory cytokines and ROS production in LPS-stimulated BV2 microglial cells. Is. (A) The expression of PDCD4 was reduced by transfection with PDCD4-shRNA plasmids. Western blot confirmed the knockdown efficiency. Since sh-PDCD4#4 had the

best inhibiting effect on PDCD4 expression, it was used in the subsequent experiments. (B) Western blot showed that knockdown PDCD4 significantly reduced the LPS-induced iNOS expression in BV2 cells. (C) RT-PCR detected the mRNA expression of iNOS, TNF-α, and IL-1β in PDCD4-knockdown BV2 cells. (E) DCFH-DA method revealed that knockdown PDCD4 largely inhibited the production of reactive oxygen species (ROS) in the LPS-stimulated BV2 cells. (*p<0.05, #p<0.05).

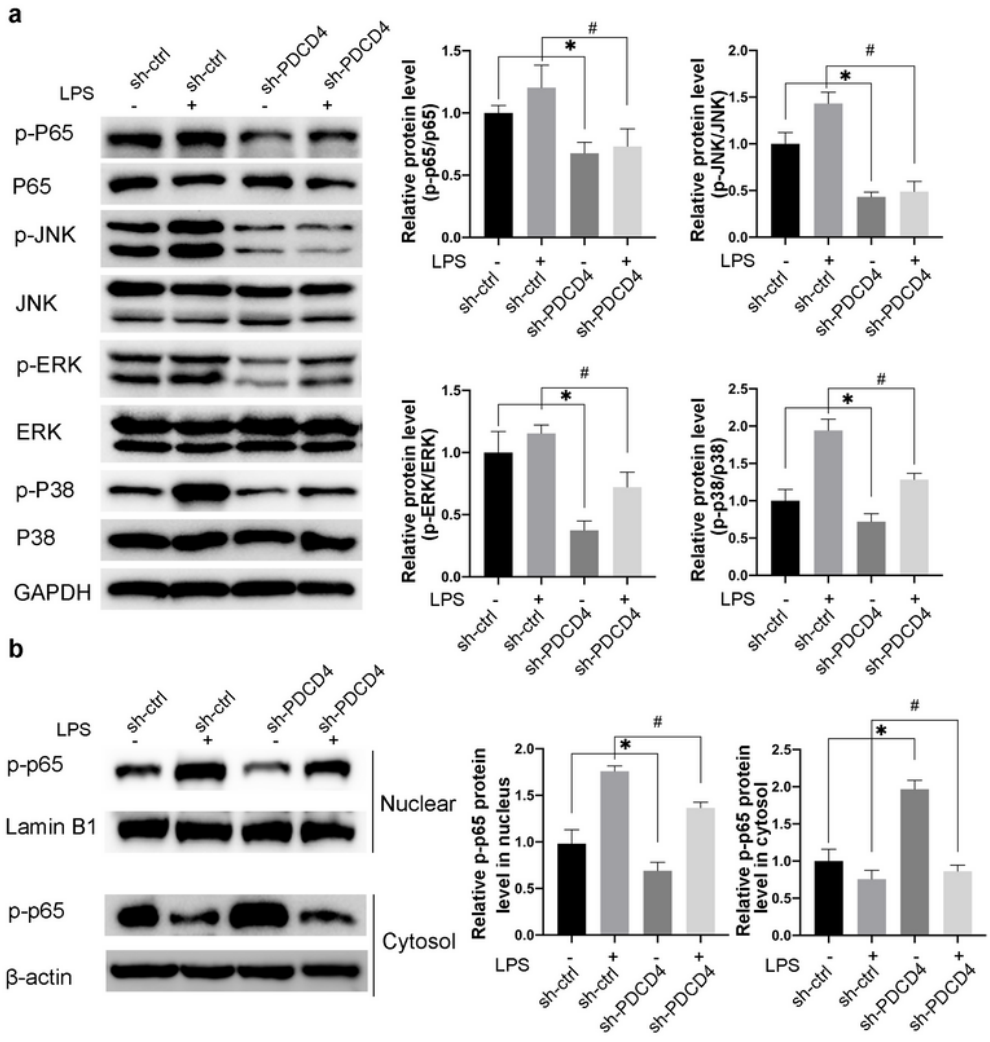

Figure 5

Silenced PDCD4 significantly inhibited the MAPK/NF-κB signaling activation in LPS-stimulated BV2 cells. (A) BV2 microglial cells were stimulated by LPS for 3 h. Western blot showed that inhibiting PDCD4 expression by shRNA significantly reduced the phosphorylation of NF-κB p65 (p-p65) and the phosphorylation of MAPKs (p-JNK, p-ERK, p-P38) in BV2 cells either with or without LPS treatment. (B) The protein levels of NF-κBp65 and p-p65 in the cytoplasm and nucleus of BV2 were also detected by western blot. (*p<0.05, #p<0.05)

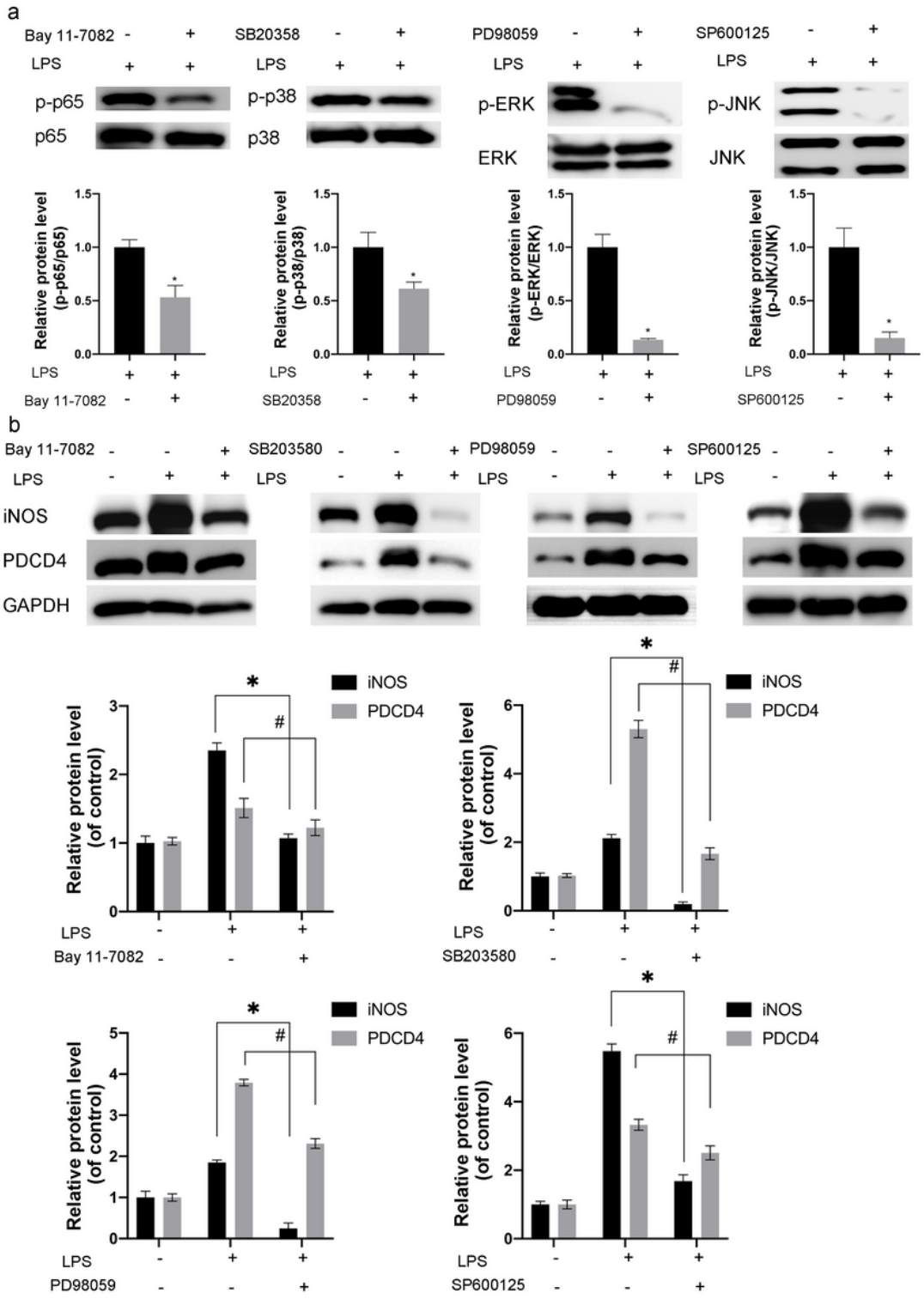

Figure 6

The expression of PDCD4 in microglia was positively regulated by MAPK/NF-κB signaling.. (A) BV2 cells were pre-treated with p65 inhibitor Bay11-7082 (20 μM), p38 inhibitor SB203580 (40 μM), ERK inhibitor PD98059, or JNK inhibitor SP600125 for 1 h, followed by LPS-stimulation for 3 h. Western blot analysis confirmed the inhibitory effect on the phosphorylation of p65, p38, ERK, or JNK. (B) The protein expression of iNOS and PDCD4 was analyzed by western blot. The LPS-stimulated PDCD4 expression in BV2 cells was largely reduced by the above inhibitors. (*p<0.05, #p<0.05)

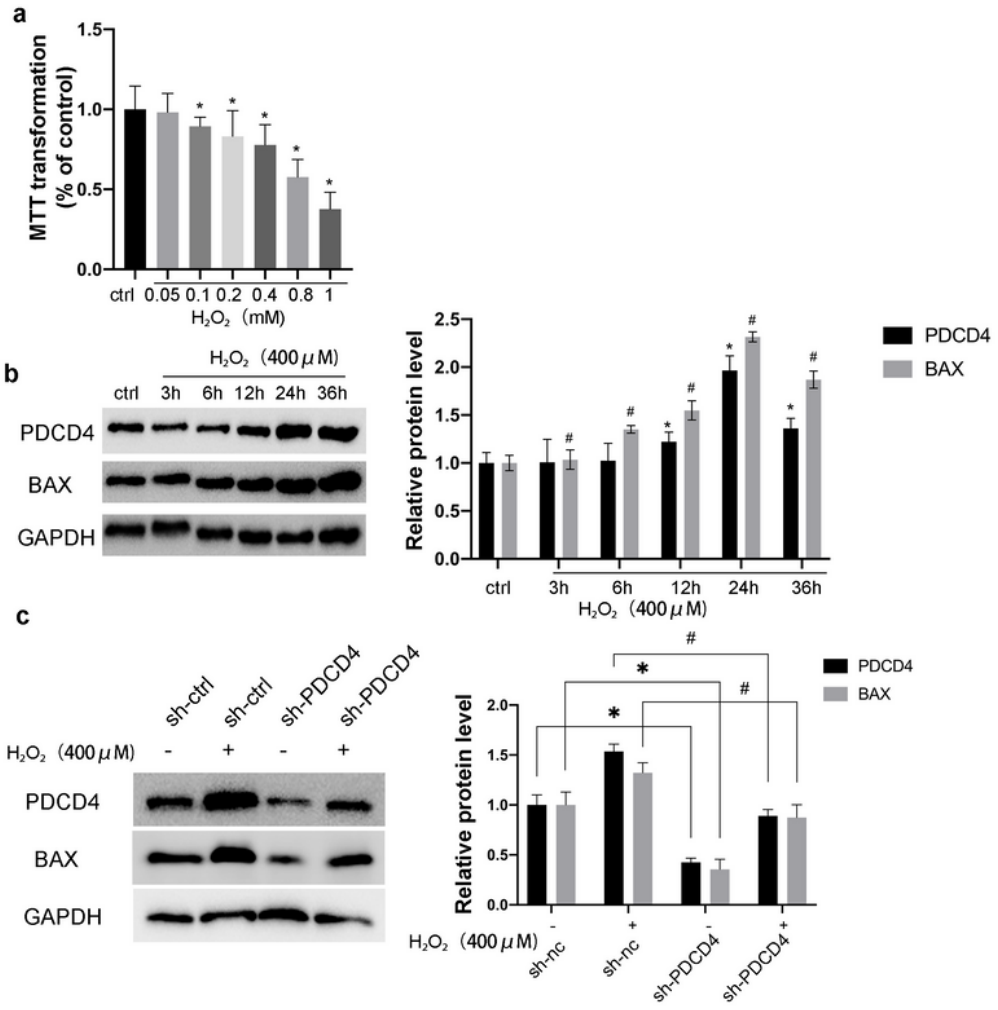

Figure 7

Silencing PDCD4 attenuated the hydrogen peroxide (H_2O_2)-induced apoptosis of HT22 neuron cells. (A) The mouse hippocampal neuron cell line HT22 was treated with different concentrations of H_2O_2 (50 μM, 100 μM, 200 μM, 400 μM, 800 μM, 1000 μM) for 24 h. The MTT assay detected the concentration-dependent decline in cell viability in H_2O_2-treated HT22 cells. (B) We selected 400 μM H_2O_2 for the following experiments to establish the neuronal apoptotic experimental model. Western blot analysis demonstrated a time-dependent increase in both PDCD4 and the proapoptotic protein Bax. (C) Silencing PDCD4 by shRNA significantly inhibited the H_2O_2-induced BAX expression in HT22 cells. (*$p<0.05$, #$p<0.05$).